Tropical–North Pacific Climate Linkages over the Past Four Centuries*

ROSANNE D'ARRIGO,[+] ROB WILSON,[#] CLARA DESER,[@] GREGORY WILES,[&] EDWARD COOK,[+]
RICARDO VILLALBA,[**] ALEXANDER TUDHOPE,[#] JULIA COLE,[++] AND BRADDOCK LINSLEY[##]

[+] *Tree-Ring Laboratory, Lamont-Doherty Earth Observatory, Palisades, New York*
[#] *School of GeoSciences, Grant Institute, Edinburgh University, Edinburgh, United Kingdom*
[@] *NCAR, Boulder, Colorado*
[&] *The College of Wooster, Wooster, Ohio*
[**] *IANIGLA, Mendoza, Argentina*
[++] *Department of Geosciences, The University of Arizona, Tucson Arizona*
[##] *Program in Geological Sciences, Department of Earth and Atmospheric Sciences, The University at Albany, State University of New York, Albany, New York*

(Manuscript received 2 December 2004, in final form 6 May 2005)

ABSTRACT

Analyses of instrumental data demonstrate robust linkages between decadal-scale North Pacific and tropical Indo-Pacific climatic variability. These linkages encompass common regime shifts, including the noteworthy 1976 transition in Pacific climate. However, information on Pacific decadal variability and the tropical high-latitude climate connection is limited prior to the twentieth century. Herein tree-ring analysis is employed to extend the understanding of North Pacific climatic variability and related tropical linkages over the past four centuries. To this end, a tree-ring reconstruction of the December–May North Pacific index (NPI)—an index of the atmospheric circulation related to the Aleutian low pressure cell—is presented (1600–1983). The NPI reconstruction shows evidence for the three regime shifts seen in the instrumental NPI data, and for seven events in prior centuries. It correlates significantly with both instrumental tropical climate indices and a coral-based reconstruction of an optimal tropical Indo-Pacific climate index, supporting evidence for a tropical–North Pacific link extending as far west as the western Indian Ocean. The coral-based reconstruction (1781–1993) shows the twentieth-century regime shifts evident in the instrumental NPI and instrumental tropical Indo-Pacific climate index, and three previous shifts. Changes in the strength of correlation between the reconstructions over time, and the different identified shifts in both series prior to the twentieth century, suggest a varying tropical influence on North Pacific climate, with greater influence in the twentieth century. One likely mechanism is the low-frequency variability of the El Niño–Southern Oscillation (ENSO) and its varying impact on Indo-Pacific climate.

1. Introduction

The existence of North Pacific interdecadal climatic variability is well documented over the past century from analyses of instrumental data (e.g., Mantua et al. 1997; Mantua and Hare 2001; Labeyrie et al. 2003). One possible mechanism for this variability is internal forcing of the northern North Pacific climate system (e.g., Nakamura et al. 1997). Alternatively, an increasing number of analyses also indicate coherent relationships between indices of higher-latitude Pacific and tropical climate (Trenberth and Hurrell 1994; Minobe 1997; Zhang et al. 1998), leading some to conclude that Pacific decadal variability (PDV) is a basinwide phenomenon that originates in the Tropics (Garreaud and Battisti 1999). Recently, Deser et al. (2004) found further support for the concept that the Tropics play a key role in North Pacific interdecadal climatic variability using a comprehensive, physically based analysis of twentieth-century observational datasets [including tropical Indo-Pacific sea surface temperatures (SSTs), rainfall, cloudiness, and sea level pressure (SLP)]. This evidence includes identification of robust linkages between interdecadal fluctuations (e.g., twentieth-century regime shifts) in the North Pacific index (NPI; Trenberth and

* Lamont-Doherty Earth Observatory Contribution Number 6799.

Corresponding author address: Rosanne D'Arrigo, Tree-Ring Laboratory, Lamont-Doherty Earth Observatory, 61 Rte. 9W, Palisades, NY 10964.
E-mail: rdd@ldeo.columbia.edu

Hurrell 1994) and several key tropical climate indices in boreal winter.

The dominant mode of wintertime atmospheric circulation variability over the North Pacific is characterized by changes in the strength of the Aleutian low pressure cell. The NPI is a robust index of this mode, which is used to track the state of cool season North Pacific SLP variability. It is defined as the area-averaged SLP over the region 30°–65°N, 160°E–140°W (Trenberth and Hurrell 1994). The NPI is closely associated with the Pacific–North America (PNA) teleconnection pattern, the dominant pattern of midtropospheric circulation variability, which extends from the North Pacific downstream over North America (Trenberth and Hurrell 1994). Negative (positive) NPI values correspond to a deeper-than-normal (less intense) Aleutian low, strengthened southerly (northerly) flow over the eastern Pacific, and warmer (cooler) temperatures along the western coast of North America (Trenberth and Hurrell 1994). The NPI shows clear evidence for multidecadal climate regimes, with primarily positive values from 1900–24 and 1947–76, and primarily negative values from 1925–46 and 1977–2003. These regimes are also evident in the Pacific decadal oscillation (PDO), the dominant mode of Pacific SST variability north of 20°N (Mantua et al. 1997). Particularly noteworthy is the pronounced 1976 regime shift (Ebbesmeyer et al. 1991; Graham 1994), which has also been identified in tropical Pacific climate and ENSO-related data. Other twentieth-century regime shifts are not as clearly related to ENSO (Deser et al. 2004).

Limitations in our understanding of the behavior of PDV result, in part, from the shortness of the instrumental record, while similar limitations in understanding of the causes and mechanisms of PDV are related to a broader suite of process issues (e.g., tropical versus extratropical air–sea interactions, lagged dynamic ocean responses to atmospheric forcing, etc.). There are not sufficient instrumental data to support any of the hypothetical models proposed to explain PDV, nor to determine how representative the twentieth-century changes are relative to long-term behavior unforced by greenhouse gases. Additional paleoclimate indices for certain key data-sparse locations (e.g., the tropical Indo-Pacific and western equatorial Pacific regions) are therefore needed for studies of PDV and identification of North Pacific–tropical linkages (Deser et al. 2004). A significant relationship between a 194-yr $\delta^{18}O$ coral record for the far western Indian Ocean [1801–1994, Malindi Marine Park, 3°S, 40°E (Cole et al. 2000); see below], and an optimal tropical climate index [the leading principal component of six normalized tropical climate series, explaining 64% of the overall variance (Deser et al. 2004)] suggested the potential for extending available information on tropical–North Pacific linkages into the past.

Herein we use tree-ring records from the land areas surrounding the North Pacific as well as coral data spanning the tropical Indo-Pacific region to extend our knowledge of tropical–North Pacific interdecadal climate linkages prior to the instrumental period. Recent efforts have substantially improved the spatial and temporal coverage of well-dated, high-resolution proxy records (tree rings and corals) for these regions [e.g., for the North Pacific: Davi et al. (2002), D'Arrigo et al. (2004), and Jacoby et al. (2004); e.g., for the Tropics: D'Arrigo et al. (1994), Charles et al. (1997), Isdale et al. (1998), Guilderson and Schrag (1999), Cole et al. (2000), Linsley et al. (2000), Urban et al. (2000), Cobb et al. (2001), Tudhope et al. (2001), Charles et al. (2003), and Linsley et al. (2004); also see Labeyrie et al. (2003)]. Yet, coverage is still very limited for vast areas, particularly for the Tropics where the existing tree-ring data network is sparse but expanding (more information available online at http://www.ldeo.columbia.edu/res/fac/trl.). Regardless, the presently available data coverage allows initial evaluation of large-scale atmosphere–ocean circulation changes across much of the Indo-Pacific region over the past several centuries.

Tree rings have been used previously to reconstruct features of North Pacific decadal climate variability, including SSTs (D'Arrigo et al. 1999), coastal air temperatures (Wiles et al. 1998), and the PDO (Biondi et al. 2001; D'Arrigo et al. 2001; Gedalof and Smith 2001; Cook 2003). Yet, there have been few attempts to describe long-term relationships between North Pacific variations and aspects of tropical climate prior to the instrumental period. Such efforts have the potential to yield insights of much value for the modeling and prediction of Pacific decadal variability (e.g., Percival et al. 2001). In perhaps the first such studies, Villalba et al. (2001, 2003) demonstrated correlations between tree-ring records from western North and South America, and related these records to Pacific basin SSTs. Evans et al. (2001) observed coherency between tree-ring records from the western Americas and a coral Sr/Ca record from Rarotonga in the equatorial Pacific, and Graham (2004) related tropical South American proxies to those from the southwestern United States. Gedalof et al. (2002), by combining five proxy records (coral and tree-ring based) of North Pacific climate variability, found evidence for basin-scale coherence in PDV and also for a robust tropical–extratropical link. In this paper we continue the examination of the North

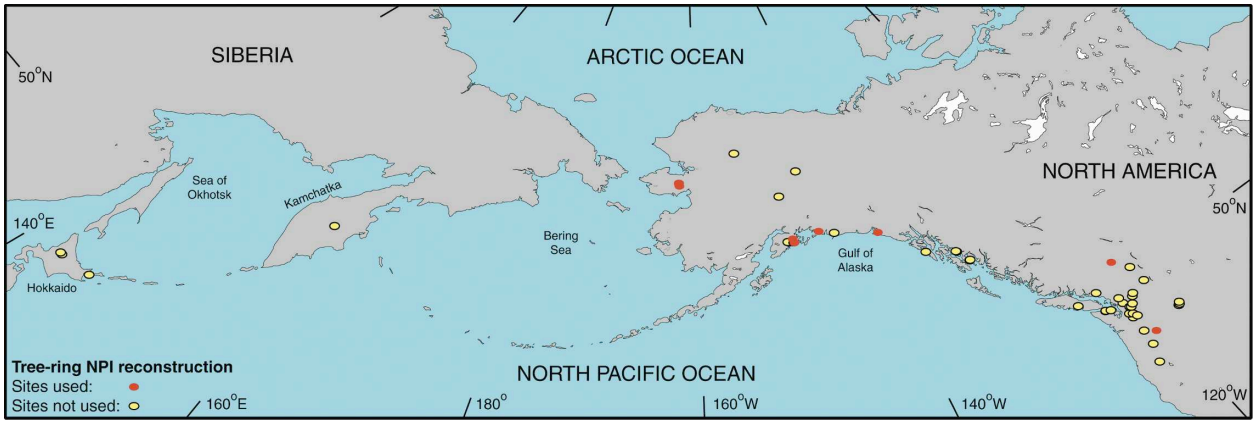

FIG. 1. Map of the North Pacific region showing locations of tree-ring sites (yellow) used as candidate predictors of the NPI. Sites in red are those included in the regression model used to reconstruct the NPI. Some dots represent more than one site.

Pacific–tropical climate connection using an extended tree-ring-based time series of North Pacific atmospheric circulation and a large-scale coral dataset from across the low-latitude Indo-Pacific region. In so doing, we further explore the large-scale linkages of decadal variability prior to the twentieth century.

2. NPI tree-ring reconstruction

To develop an extended record of North Pacific decadal-scale atmospheric circulation changes that could readily be compared to tropical climate indices, we reconstructed the NPI of Trenberth and Hurrell (1994) using tree-ring data. To this end, 67 chronologies from the land areas surrounding the North Pacific rim (Fig. 1) were used as candidate predictors in principal component (PC) regression analysis (Cook et al. 1999). The chronologies selected for modeling of the NPI are all mainly temperature-sensitive records of coniferous tree species from the northeastern North Pacific, primarily from the Gulf of Alaska and Pacific Northwest regions. Some of these records were used previously to reconstruct the PDO (D'Arrigo et al. 2001; Cook 2003). Tree-ring records from precipitation-sensitive lower-latitude western North American sites, also used to reconstruct the PDO (D'Arrigo et al. 2001; Cook 2003), were not included in the NPI modeling as we were primarily interested in identifying distinct linkages between North Pacific and tropical climate. Using the 1900–83 common period, correlations were calculated between the chronologies and the monthly NPI over an 18-month interval beginning in May of the year prior to growth and ending in October of the current growth year (Fritts 1976). Of the 67 chronologies, 18 (red dots in Fig. 1) correlated significantly at or above the 90% significance level for the winter/spring months of the NPI and were thus retained for further analysis. From a principal component analysis (PCA), only those eigenvectors showing eigenvalues >1 were retained for regression (Cook and Kairiukstis 1990).

To develop the longest possible reconstruction, we used a nested approach (e.g., Meko 1997; Cook et al. 2002) in which the number of available chronologies declines back in time (Fig. 2). For this purpose, a PC regression model was first developed using all of the available data, resulting in the most robust reconstruction. A second nest is based on the next common period of all series with the shortest series removed, and so on. For each nested subset of variables, a reconstruction is developed and separate calibration and verification statistics are made for both early (1900–40) and late (1941–83) periods of calibration. This allows for a good measure of the loss in signal fidelity in the reconstruction back in time. To create the final reconstructed time series, the relevant "sections" from each full-period (1900–83) calibrated nested model are spliced together. This is done after the mean and variance of each nested time series are adjusted to that of the fully replicated nested reconstruction so that there are no changes in variance in the time series due to weakening in the modeled signal. For this study, three nested subsets were used to generate the NPI tree-ring reconstruction (starting from 1600, 1629, and 1762, respectively). Due to lower levels of statistical validation, the earlier part of the reconstruction, based on less data from the least replicated nest, should thus be viewed with greater uncertainty. The best regression model was found for the December–May season (Fig. 2a), which accounts for 41% of the variance in the instrumental NPI for the most replicated nest. Most of the variance in the NPI is

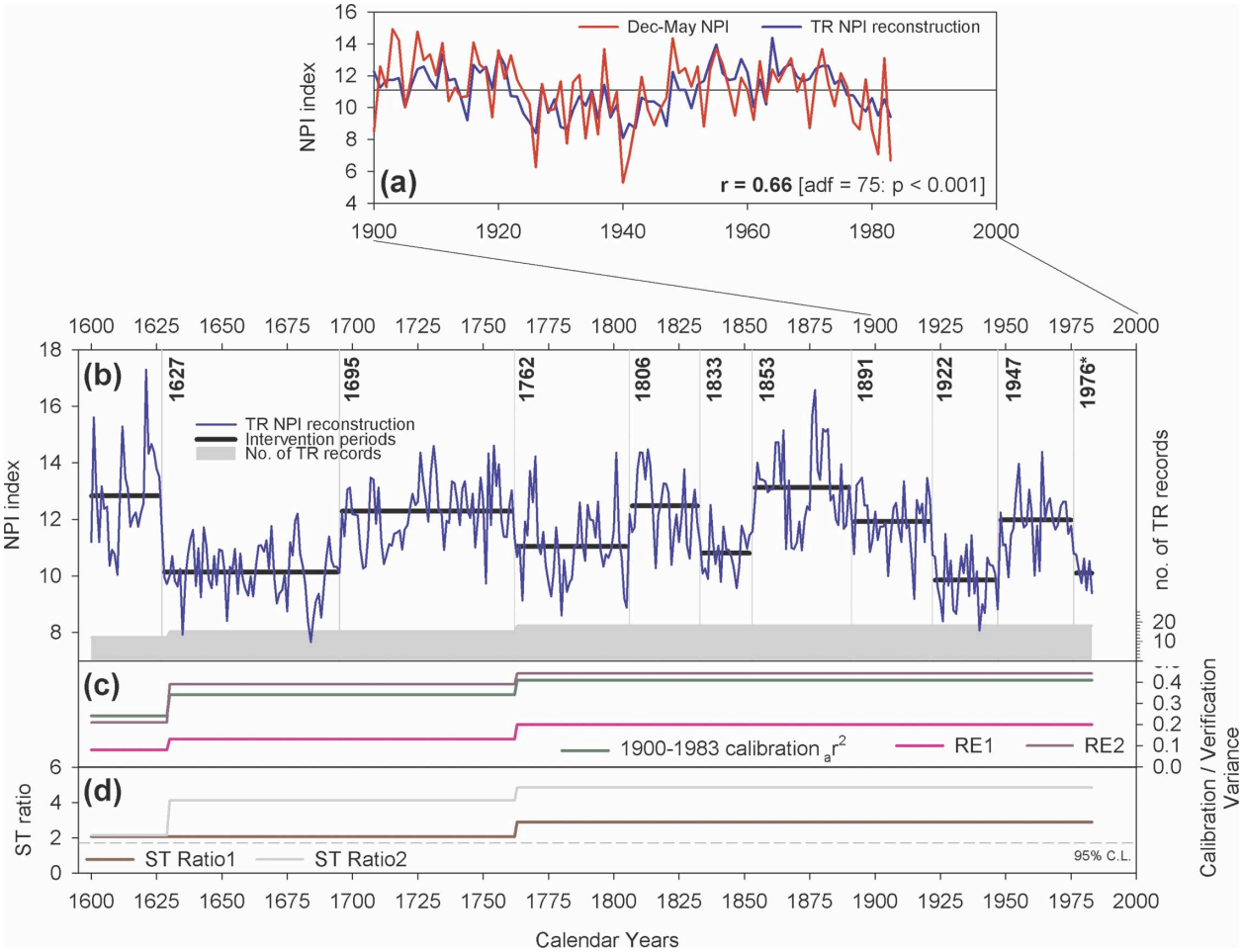

FIG. 2. Tree-ring based NPI reconstruction. (a) Actual and estimated Dec–May NPI for the 1900–83 calibration period: Adf = adjusted degrees of freedom. The degrees of freedom were adjusted to account for the autocorrelation in the data so that significance of the correlations could be assessed (Trenberth 1984). (b) Reconstruction of the Dec–May NPI from A.D. 1600–1983 based on North Pacific tree-ring data. The highlighted phase shifts were identified using intervention analysis (significant at the 90% confidence limit). Asterisk (*) indicates the 1976 shift was identified in the actual Dec–May NPI series as there are too few observations after 1976 to identify a significant shift in the reconstruction. (c) Nested calibration (1900–83 $_a r^2$) and RE results through time. The $_a r^2$ is the level of explained variance after adjustment for degrees of freedom. The RE is a measure of the common variance between the actual series and the tree-ring estimates, for which a positive value indicates skill in the regression. RE1 (RE2) shows the RE value for the 1941–83 (1900–40) verification period after calibration on the 1900–40 (1941–83) period, calculated for each nest. (d) The sign test (ST) ratio (positive agreements divided by negative agreements) verification results through time. The ST, which measures how well the reconstructed estimates track the year to year variations in the instrumental data (Fritts 1976; Cook and Kairiukstis 1990), shows that all nested models pass verification.

in the colder months, and this selected season includes the December–March period of strongest atmospheric circulation variability in the North Pacific (Trenberth and Hurrell 1994). The correlation between the December–May and December–March seasons is 0.95 over the 1900–2002 period.

Calibration and verification tests (Cook and Kairiukstis 1990) indicate that the reconstruction model provides reasonably valid estimates of past NPI variability (Figs. 2c and 2d). Cross-validation tests include positive reduction of error (RE) statistics, which indicate predictive skill in the reconstruction (Gordon and LeDuc 1981) and significant sign test (ST; Fritts 1976) results, that indicate that the tree-ring estimates successfully capture the interannual variability present in the instrumental NPI data. The tree-ring based December–May NPI reconstruction (TR NPI), dating from A.D. 1600–1983, is presented in Fig. 2b. An intervention analysis (Box and Tiao 1975), which is essentially a two-sample *t* test that can be applied to autocorrelated data, was applied to the NPI reconstruction to identify significant shifts in the series. This analysis was made by compar-

ing the mean values of 15-yr periods on either side of each year throughout the series. While interventions can take many forms, we tested only for step interventions. This method is similar to that used by Mantua et al. (1997) and Gedalof and Smith (2001) for identifying shifts in the PDO.

The NPI reconstruction successfully tracks the known regime shifts (1924/25, 1946/47, and 1976/77) seen in the instrumental NPI during the twentieth century (Trenberth and Hurrell 1994; Deser et al. 2004), although the mid-1920s shift appears to predate the instrumental record by 2 yr. Although the quality of the TR NPI decreases back in time (Fig. 2c), it indicates that prior to the instrumental period there are decadal-scale variations that may also represent regime shifts. Significant "shifts" (at the 90% confidence limit) are identified in 1627, 1695, 1762, 1806, 1833, 1853, and 1891. Comparison of the three nested time series (not shown) indicates that the identified 1627 and 1762 shifts, which roughly equate to the start of the two recent nests, are not artifacts of the nesting procedure.

To help assess the relationship between the TR NPI reconstruction and Indo-Pacific climate, Figs. 3a and 3b present maps that compare the spatial correlations of December–May SST anomalies (Kaplan et al. 1998) with the tree-ring reconstructed and instrumental NPI records for the common interval 1900–83. The correlations are based on 9-yr low-pass-filtered data to emphasize the relationships on decadal time scales. The maps show similar patterns of December–May SST anomalies, indicating that the reconstruction captures the dominant spatial features of the North Pacific–tropical climate relationship during this period.

3. Coral-based Indo-Pacific Ocean tropical index reconstruction

As a logical extension of the analysis made by Deser et al. (2004), we next compared the TR NPI reconstruction to tropical climate proxy data to extend our information on tropical–North Pacific linkages prior to the twentieth century. As noted, Deser et al. (2004) presented significant correlations between an $\delta^{18}O$ coral record from the western Indian Ocean [Malindi Marine Park, 3°S, 40°E (Cole et al. 2000)] and an optimal tropical climate index (OTI) based on instrumental Pacific and Indian Ocean SST, rainfall in the South Pacific convergence zone, cloud cover in the central equatorial Pacific, and SLP in the Pacific and Indian Oceans. Herein, we expand upon this analysis and identify 12 coral proxy records from the Pacific and Indian Oceans that correlate significantly with this index. We then develop an independent large-scale reconstruction of the OTI from these records for comparative analysis.

From the National Oceanic and Atmospheric Administration (NOAA) Paleoclimatology Program and unpublished sources, there are more than 50 annually to monthly resolved coral records that are ≥100 yr in length, representing a variety of coral proxy types (e.g., calcification, $\delta^{18}O$, Sr/Ca, U/Ca, Ba/Ca, and fluorescence data). Correlation analysis of annual (January–December) time series identifies 12 coral records that covary with the OTI at or above the 95% significance level (Fig. 3c). Eleven of these coral time series are records of skeletal $\delta^{18}O$ (a proxy that records the combined effects of temperature and salinity changes during the growth of the coral). The other coral time series (HVI) is a record of skeletal fluorescence, which in this case is viewed as a rainfall and river runoff proxy. Despite the potential additional influence of salinity changes on coral skeletal $\delta^{18}O$, most of these records are reported to portray significant correlations with local SSTs (although there are also salinity effects). All are also noted to show strong synoptic-scale climate signal relationships with either ENSO or its teleconnections (Allan 2000). It is therefore not surprising, due to the noted large-scale coherence of decadal-scale variability across the Indo-Pacific region (e.g., Trenberth and Hurrell 1994; Mantua et al. 1997; Deser et al. 2004), that these records correlate well (based on unfiltered data) with the OTI. The locations of these 12 coral series clearly fall within the regions where SST anomalies are well correlated (positively) with the OTI; note also that the sign (negative) of the coral record correlations with the OTI (Fig. 3) is consistent with those of the inverse relationship between coral $\delta^{18}O$ and SST.

Following the same method utilized for the development of the TR NPI reconstruction, nested principal component regression was used to develop an independent coral-based OTI reconstruction. The coral OTI reconstruction is compared with the actual OTI series in Fig. 4a. Fifty-six percent of the OTI variance is explained by the most replicated nest, which decreases to 33% for the 1781–1800 three-series model (Fig. 4c). Split-period calibration–verification of each nested model [calibration made over the 1900–43 (1944–86) period and verified over 1944–86 (1900–43)] indicates model skill with positive RE values for all nests back to 1801 (Fig. 4c). The sign test marginally fails for the 1900–43 period for the nests prior to 1881. It is likely that the failure of the reconstruction prior to 1801 reflects the fact that the Malindi (MAL) record, from the far western Indian Ocean (Fig. 3c), is not in the input matrix prior to this period. The earliest three-series nest did not utilize PC regression as the use of PCA on so few records is not a valid approach. Rather, the se-

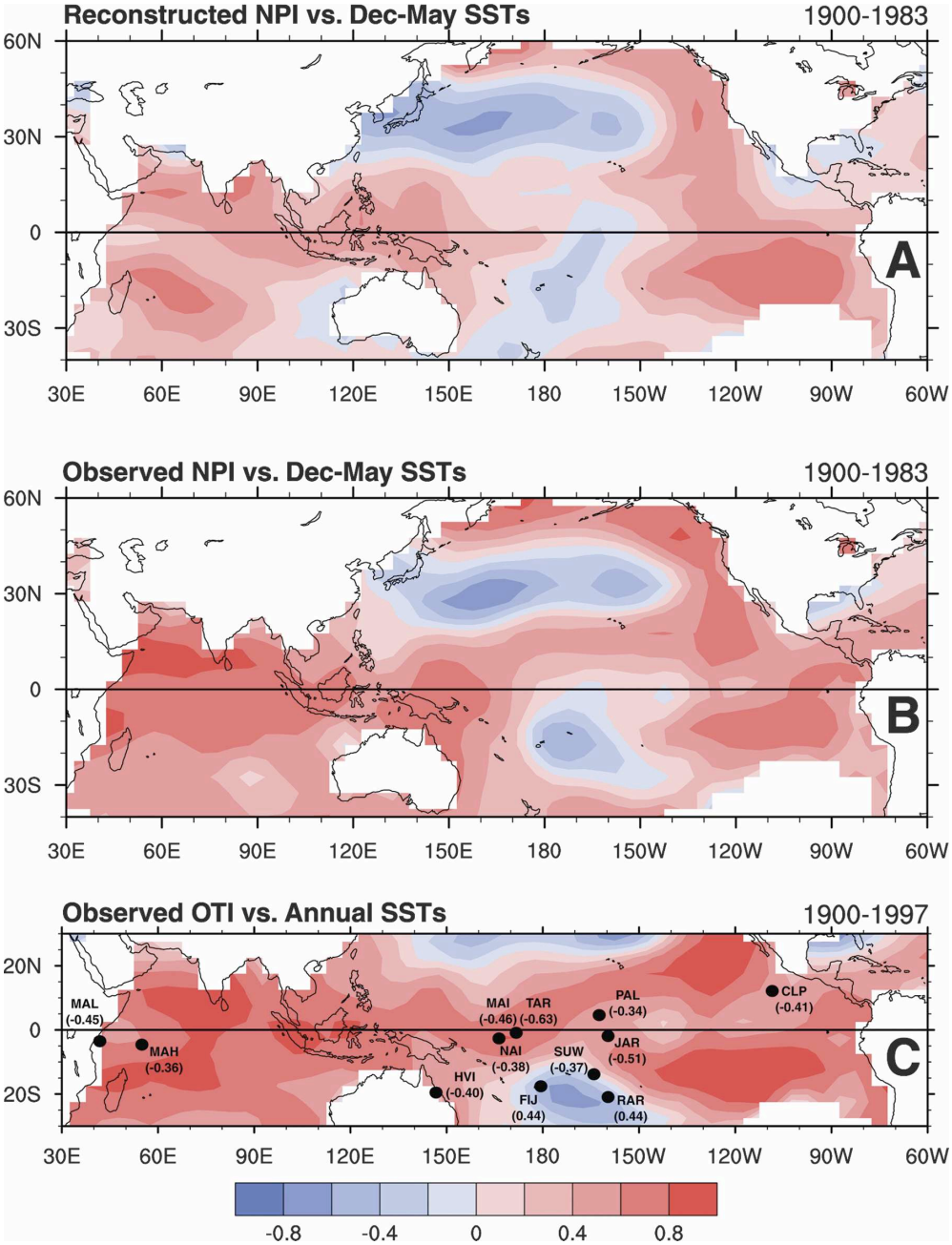

FIG. 3. Spatial correlation plots. (a) Reconstructed and (b) actual NPI (inverted sign) compared to Dec–May Pacific and Indian Ocean SST fields (Kaplan et al. 1998) for 1900–83. (c) OTI (Deser et al. 2004) compared to annual SST anomalies over the period 1900–97. The contour interval is 0.2. The contoured correlations only provide a guide to indicate that we are capturing the large-scale signal. All spatial correlations were made using low-pass-filtered (9 yr) data. Coral records are shown that correlate significantly (95% confidence limit), using unfiltered data, after taking into account autocorrelation in the non-filtered time series (Trenberth 1984). Correlations for the 1900–86 period are shown in parentheses: MAL, Malindi (1801–1992; Cole et al. 2000); MAH, Mahe, Seychelles (1846–1995; Charles et al. 1997); HVI, Havannah Island (1644–1986, Isdale et al. 1998); NAI, Nauru Island (1897–1994; Guilderson and Schrag 1999); MAI, Maiana (1840–1994; Urban et al. 2000); TAR, Tarawa (1894–1988; Cole and Fairbanks 1990; Cole et al. 1993); PAL, Palmyra Island (1886–1996; Cobb et al. 2001); FIJ, Fiji (1781–1996; Linsley et al. 2004); RAR, Rarotonga (1726–1996; Linsley et al. 2004); JAR, Jarvis (1850–1998; A. W. Tudhope et al. 2005, unpublished manuscript); SUW, Suwarrow Atoll (1881–1998; A. W. Tudhope et al. 2005, unpublished manuscript); and CLP, Clipperton Atoll (Linsley et al. 2000). All coral records are $\delta^{18}O$ except HVI, which is fluorescence.

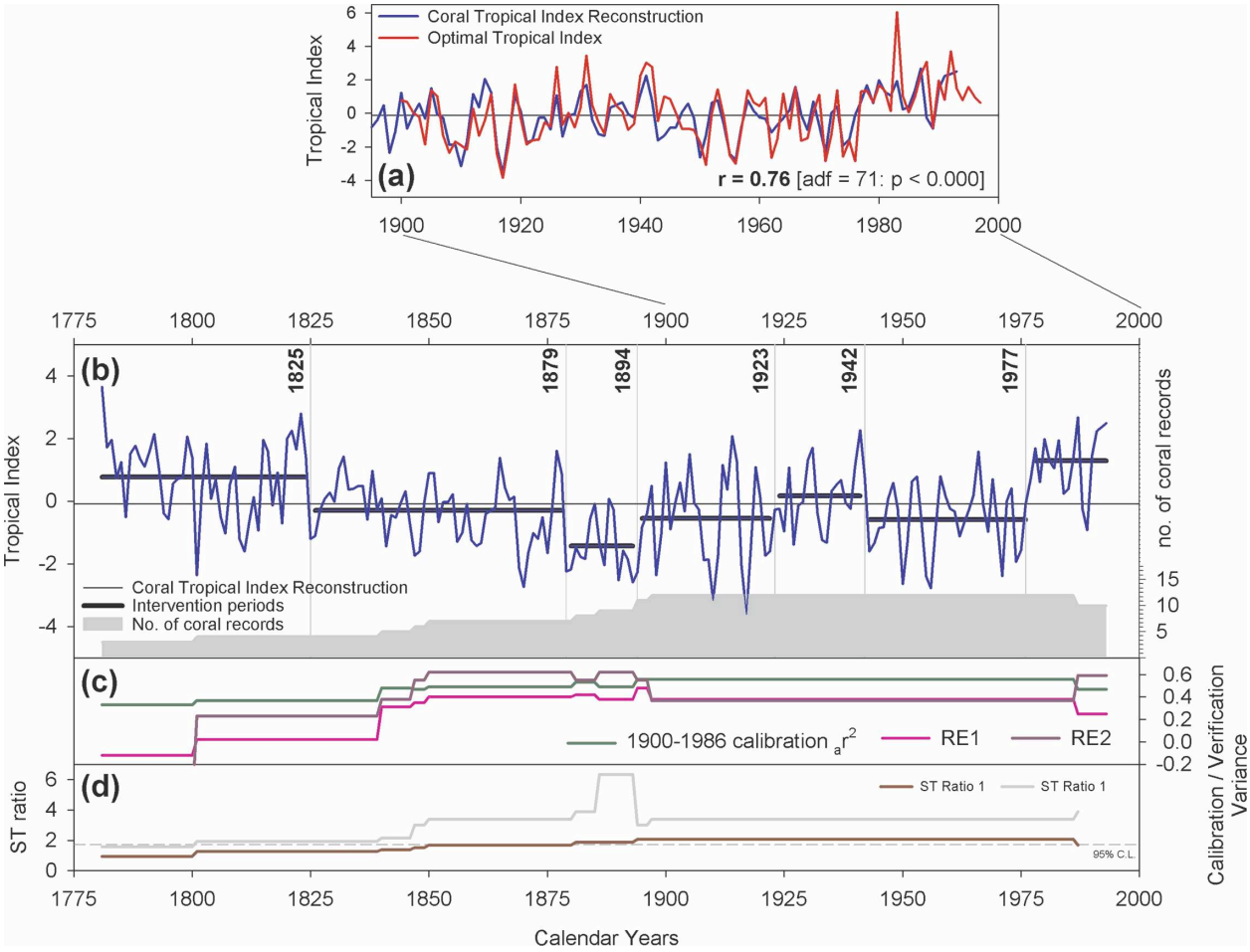

FIG. 4. Coral-based reconstruction of the Deser et al. (2004) OTI. (a) Actual and estimated OTI series for the 12 coral series nested PC regression model; adf is the adjusted degrees of freedom. The degrees of freedom were adjusted to account for the autocorrelation in the data so that significance of the correlations could be assessed (Trenberth 1984). (b) The full coral OTI reconstruction. The highlighted phase shifts were identified using an intervention analysis (significant at the 90% confidence limit). (c), (d) As in Fig. 2 except full calibration is over the 1900–86 period and split-period calibration–verification are made over the 1900–43 and 1944–86 periods. The reconstruction is well calibrated and verified back to 1801, except that the ST ratio is slightly below the 95% confidence limit for the 1900–43 verification period prior to 1881. The earliest three-series nest did not utilize PC regression. Rather, the series were entered into the regression model using a stepwise process.

ries were entered into the regression model using a stepwise process.

Intervention analysis of the OTI reconstruction successfully identifies the three climatic shifts of the twentieth century (Trenberth and Hurrell 1994; Deser et al. 2004), although it should be noted that the significance of the shifts at 1923 and 1942 are weaker than that for 1976 ($p < 0.05$) and are only significant at the 90% confidence limit. Prior to the known twentieth-century shifts, the intervention analysis identifies significant shifts at 1825, 1879, and 1894 (Fig. 4b). As with the TR NPI series, less confidence is advised when interpreting these earlier shifts, as the fidelity of the reconstruction decreases back in time (Figs. 4c and 4d) due to the decreasing number of coral records (Fig. 4b).

4. Comparison of tropical and extratropical reconstructions

Figure 5 compares the TR NPI and coral OTI reconstructions. Running correlations show that the two series correlate significantly (note that the sign of the OTI reconstruction has been reversed) for most of the twentieth century, but prior to the calibration period correlations are generally not significant, except for the early nineteenth century where coherence is similar in strength and sign to that of the twentieth century. We note that the period of weaker correlation (centered in the mid- to late nineteenth century) appears to coincide with a period of generally weaker interannual variance in the OTI reconstruction, suggesting that this may be a

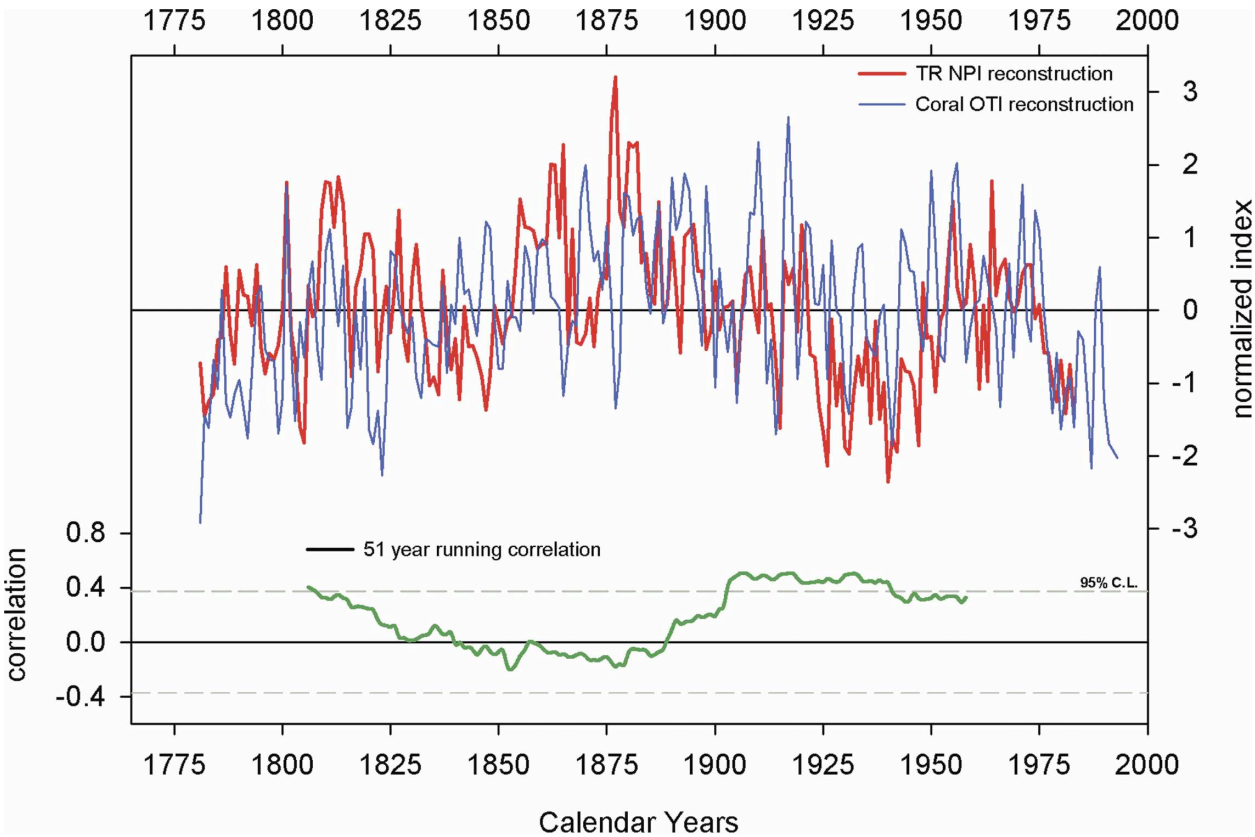

FIG. 5. (top) Comparison of the TR NPI and coral OTI reconstructions. Both series have been normalized to their common period while the sign of the coral OTI series has been reversed to aid comparison. (bottom) Running 51-yr correlations between both series. The 95% confidence limits have been adjusted to take into account the autocorrelation in the time series (Trenberth 1984).

factor in determining the strength of the correlation between these annually resolved time series. A cross-spectral analysis (Mann and Lees 1996) was also performed to compare the OTI and NPI reconstructions (not shown). It reveals statistically significant (95%–99% level) coherency between the two series (for the common period from 1745 to 1783) on interannual to decadal time scales, including the broader ENSO bandwidth (2–11 yr; Allan 2000).

Relationships between the NPI and ENSO-related indices (tropical Pacific SSTs and the Southern Oscillation index or SOI) were previously evaluated for the recent instrumental period (e.g., Trenberth and Hurrell 1994; Deser et al. 2004). In Fig. 6 we extend this assessment with a comparison and running correlation between the TR NPI and coral OTI series and an independent reconstruction of Niño-3 SSTs based on a multiproxy dataset that includes information on decadal to multidecadal variability (Mann et al. 2000). Similar patterns of correlation were observed by comparing the TR NPI and coral OTI reconstructions to a largely independent reconstruction of the SOI based primarily on subtropical western North American tree-ring data, which has less decadal variability (Stahle et al. 1998). For the TR NPI comparison with the Mann et al. (2000) series, the sliding correlations (Fig. 6a) show varying coherence through time with significant but weak correlations around 1800–50 and significant correlations in the early twentieth century. Correlations are also significant for a brief period in the early 1700s. The sliding correlation results using the coral OTI reconstruction (Fig. 6b) indicate strong coherence with the Niño-3 reconstruction for the twentieth century ($\bar{r} = 0.72$), which declines to zero in the mid–nineteenth century. The lack of a correlation between these time series in the mid–nineteenth century is interesting given the importance of ENSO to the variance in both. One possible explanation is that the Niño-3 reconstruction appears to reflect anomalous (non-ENSO like) conditions during this period (Mann et al. 2000). Alternatively, or in addition, the importance of ENSO to variance in the OTI may weaken over this period.

The observations for the twentieth century are further explored in Table 1, in which we compare the in-

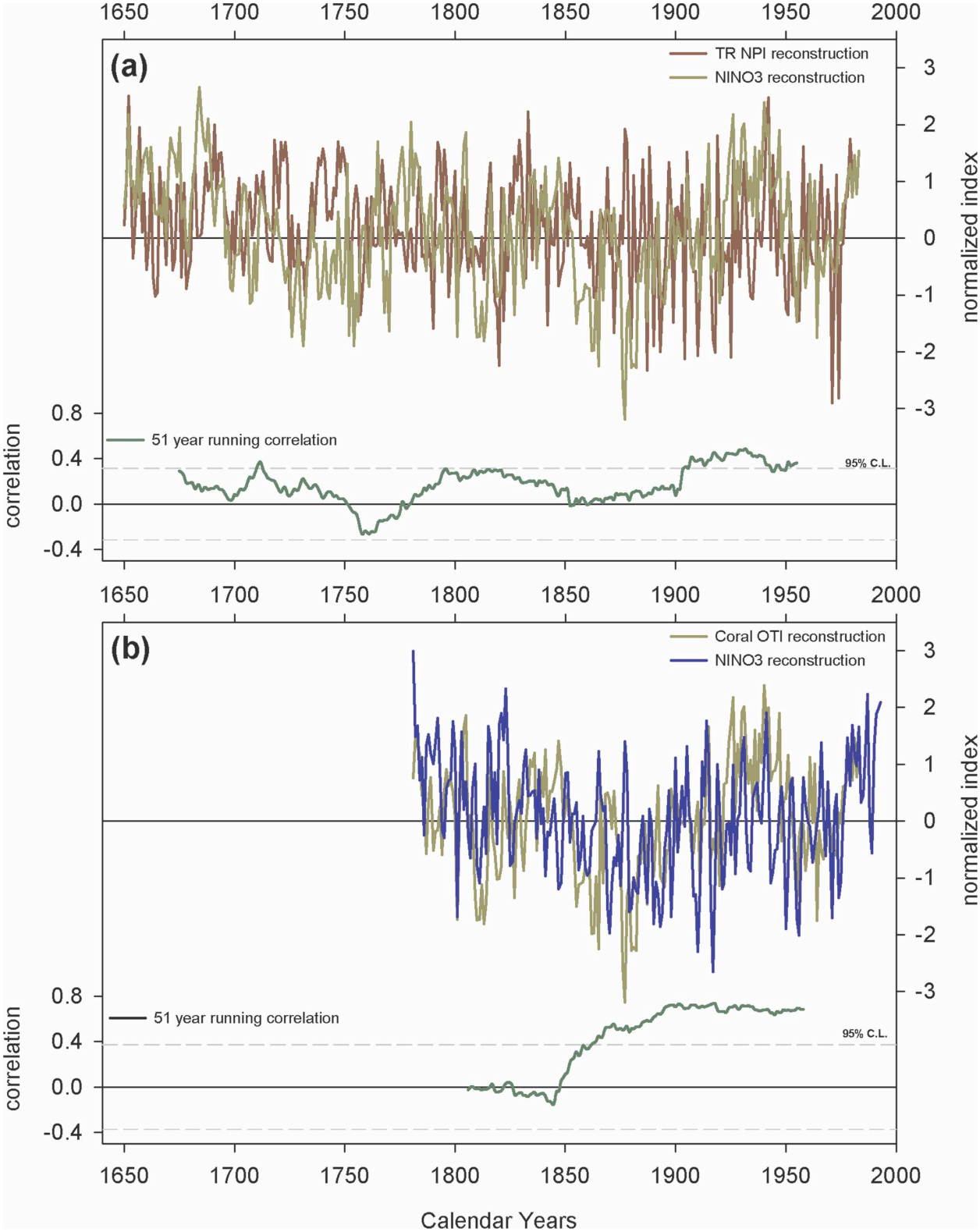

FIG. 6. (a, top) Comparison of the TR NPI (reversed sign) with the Niño-3 SST reconstruction of Mann et al. (2000). Both series have been normalized to their common period. (a, bottom) Running 51-yr correlations between both series. The 95% confidence limits have been adjusted to take into account the autocorrelation in the time series (Trenberth 1984). (b) As in (a) but for comparison between the coral OTI series and the Niño-3 reconstruction.

TABLE 1. (a) Correlation of four proxy series with climate indices related to ENSO and Indo-Pacific climate. Proxies are the NPI reconstruction (TR NPI), the coral OTI reconstruction, a reconstruction of Niño-3 SST based on multiproxy data (Mann et al. 2000), and the first eigenvector scores (PC1) of three tree-ring width chronologies of teak for Indonesia (D'Arrigo et al. 1994). The instrumental records are an index of the SOI, Niño-3 SST, Indian Ocean SST, and an index of Indian monsoon rainfall. SOI, Niño-3, and monsoon data from R. Allan, U.K. Hadley Center; Indian Ocean SST from Kaplan et al. (1998)'s analysis. (b) As in (a) except correlations are made using actual indices of the NPI (Dec–May) and the OTI of Deser et al. (2004). The unfiltered correlations were made over the 1900–83 period (except for the Niño-3 reconstruction data: 1900–80), while the filtered (three-point binomial) correlations were made over the 1901–82 period (Niño-3 reconstruction: 1901–80). Double (single) asterisks denote significance at the 95% (90%) confidence limit. The significance values have been adjusted for autocorrelation in the data (Trenberth 1984). The "optimized seasons" are those for which the highest correlation was identified in an initial screening process.

(a)

Unfiltered	SOI	Niño-3 SST	Indian SST	Monsoon index
TR NPI	0.28**	−0.38**	−0.37**	−0.05
Coral OTI	−0.69**	0.76**	0.71**	−0.20*
Niño-3 reconstruction	−0.74**	0.77**	0.73**	−0.04
PC1 teak	0.42**	−0.41**	−0.27**	0.32**
Three-point binomial	**SOI**	**Niño-3 SST**	**Indian SST**	**Monsoon index**
TR NPI	0.43**	−0.37*	−0.40	-0.06
Coral OTI	−0.75**	0.76**	0.68**	−0.41**
Niño-3 reconstruction	−0.71**	0.75**	0.71**	−0.21
PC1 teak	0.25	−0.40**	−0.13	0.31*

Optimized seasons for each proxy: SOI—NPI recon (Aug–Nov), coral OTI (Jan–Dec), Niño-3 reconstruction (Jul–Apr), teak PC1 (Jun–Dec); Niño-3 SST—NPI reconstruction (Feb–May), coral OTI (Jan–Jun), Niño-3 reconstruction (pJul–Apr), and teak PC1 (Sep–Dec); Indian Ocean SST—NPI recon (Jun–Nov), coral OTI (Jan–Dec), Niño-3 reconstruction (pNov–Aug), and teak PC1 (Oct–Dec).

(b)

Unfiltered	SOI	Niño-3 SST	Indian SST	Monsoon index
Dec–May NPI	0.44**	−0.51**	−0.53**	−0.22**
OTI	−0.76**	0.84**	0.79**	0.09
Three-point binomial	**SOI**	**Niño-3 SST**	**Indian SST**	**Monsoon index**
Dec–May NPI	0.37**	−0.57**	−0.69**	−0.06
OTI	−0.71**	0.79**	0.79**	−0.15

Optimized seasons for synoptic series: SOI—Dec–May NPI reconstruction (Dec–Apr) and tropical index (pJun–Mar); Niño-3 SST—Dec–May NPI reconstruction (Jan–May) and tropical index (pJun–May); Indian Ocean SST—Dec–May NPI reconstruction-(Mar–Sep) and tropical index (Dec–Jun).

strumental and proxy NPI and OTI to various indices of tropical Indo-Pacific climate. Correlations are presented for the NPI, OTI, and Niño-3 reconstructions (Table 1a) and actual indices of the NPI and OTI (Table 1b) against indices of ENSO and related Indo-Pacific climate (including the SOI, Niño-3 SST, Indian Ocean SSTs, and an Indian monsoon rainfall index). Also included are correlations with a teak tree-ring width record based on three chronologies from Indonesia, one of the few other high-resolution tropical proxies available for comparison (D'Arrigo et al. 1994). As expected, the TR NPI series, based only on North Pacific tree-ring data, is more weakly (but in most cases significantly) correlated with the ENSO and tropical indices than the other series. Interestingly, comparison of the coral OTI reconstruction with the ENSO-related indices reveals correlations that are comparable to those identified for the Niño-3 reconstruction (Table 1a). This result is not surprising, however, as the actual OTI series is also highly correlated with ENSO-related time series (Table 1b) and many of the coral records used for the OTI reconstruction are documented to show a strong ENSO signal. The teak record and the coral OTI reconstruction also correlate significantly with Indian monsoon rainfall (which may be a factor linking tropical and extratropical climate; see section 5), although the actual OTI series does not.

5. Discussion and conclusions

We have presented an extended tree-ring-based record of the NPI, an important index of the atmospheric circulation closely linked to the climate of the North Pacific and adjacent land areas (Trenberth and Hurrell 1994). This reconstruction shows agreement with instrumental indices of both North Pacific and tropical climate. Both the NPI reconstruction and an independently derived coral-based reconstruction of an optimal tropical climate index (OTI) for the Indian and Pacific Oceans (Deser et al. 2004) reflect the decadal-scale regime shifts of the twentieth century and support the concept of a tropical role in PDV in the recent period. Both the tree-ring- and coral-based reconstructions reveal regime shifts prior to the instrumental record, but, crucially, none appear synchronous between the two records. These shifts are generally comparable in intensity to those of the recent period although some are of even longer duration. Our analysis thus suggests that the 1976 transition was not unique in terms of magnitude, but that for some periods prior to the twentieth century, different mechanisms may have been responsible for tropical and extratropical interdecadal vari-

ability. A similar conclusion was reached in related studies of North Pacific and South American tree-ring data (e.g., Evans et al. 2001; Gedalof et al. 2002). Unlike such other studies, our report extends the paleoevidence for better assessment of a potential tropical–high-latitude connection into the Indian Ocean as well, although it should be emphasized that the coral dataset is biased to the central and western Pacific.

Changes in common variance over time could be related to the robustness of the proxies in their earlier periods. Alternatively, the varying sign and magnitude of correlations between the TR NPI and coral OTI reconstructions and Niño-3 proxy may reflect the time-varying impact of tropical forcing (e.g., ENSO, monsoon effects; Fig. 6 and Table 1) and its teleconnections on North Pacific climate. The strongest positive correlation between the tropical and North Pacific proxies is in the twentieth century. Consistent with this observation, various reconstructions of the PDO, based on North Pacific and southwestern United States tree-ring data, show greater coherency during the twentieth century (Biondi et al. 2001; D'Arrigo et al. 2001; Gedalof and Smith 2001; Cook 2003). Similarly, South Pacific coral records indicate more symmetry across the North and South Pacific after the late 1880s (Linsley et al. 2004), and there is stronger agreement between higher-latitude Pacific tree-ring data and a tropical coral record in the twentieth century, suggesting a stronger role for the Tropics at this time (Evans et al. 2001).

The relationships described by Villalba et al. (2001, 2003), Evans et al. (2001), and herein suggest basin-wide relationships linked to decadal to longer-term fluctuations of ENSO or other forcing mechanisms (e.g., Linsley et al. 2004). The significant contributions of ENSO-sensitive coral records to the coral OTI, and the frequency characteristics of this index, suggest that ENSO plays a role in low-frequency Pacific variability. However, the ephemeral correlation between the coral OTI and tree-ring NPI indicates that the importance of tropical dynamics has fluctuated in strength over the past few centuries, invoking the need for alternate (nontropical) mechanisms for multidecadal North Pacific climate shifts. The Asian monsoon may also play a key role in the transmission of climate signals between the Tropics and extratropics (Table 1; Yamagata and Masumoto 1992). Variations in the NPI may thus be a remote response to tropical Pacific forcing from precipitation via atmospheric dynamics (Deser et al. 2004). More research is needed using instrumental and proxy data from the tropical Indian Ocean as well as the Pacific sector (along with modeling and theoretical work) in order to explore this theory.

Acknowledgments. This project was funded by the National Science Foundation's Paleoclimate Program (Grants ATM02-02898 and OCE 04-02474). This project was also supported by the Inter American Institute (IAI). We thank contributors to the NOAA Paleoclimatology Data Bank. We thank Adam Phillips (NCAR) for assistance with Fig. 3. We thank Ze'ev Gedalof and one anonymous reviewer for comments that considerably improved the manuscript. Rob Wilson and Alexander Tudhope are partly funded by the European Union Project "Simulations, Observations and Palaeoclimatic data" (SOAP) and by the U.K. NERC. Clara Deser gratefully acknowledges support from the NOAA–OGP CLIVAR Program. Julia Cole is funded by a CAREER grant from the National Science Foundation and NOAA's Climate Change Data and Detection Program. Braddock Linsley is funded by NSF Grant OCE-0318296.

REFERENCES

Allan, R., 2000: ENSO and climatic variability in the past 150 years. *El Niño and the Southern Oscillation: Multiscale Variability and Global and Regional Impacts*, H. Diaz and V. Markgraf, Eds., Cambridge University Press, 3–56.

Biondi, F., A. Gershunov, and D. Cayan, 2001: North Pacific decadal climate variability since AD 1661. *J. Climate,* **14,** 5–10.

Box, G. E. P., and G. C. Tiao, 1975: Intervention analysis with applications to economic and environmental problems. *J. Amer. Stat. Assoc.,* **70,** 70–79.

Charles, C. D., D. E. Hunter, and R. G. Fairbanks, 1997: Interaction between the ENSO and the Asian monsoon in a coral record of tropical climate. *Science,* **277,** 925–928.

——, K. Cobb, M. D. Moore, and R. G. Fairbanks, 2003: Monsoon–tropical ocean interaction in a network of coral records spanning the 20th century. *Mar. Geol.,* **201,** 207–222.

Cobb, K. M., C. D. Charles, and D. E. Hunter, 2001: A central tropical Pacific coral demonstrates Pacific, Indian, and Atlantic decadal climate connections. *Geophys. Res. Lett.,* **28,** 2209–2212.

Cole, J. E., and R. G. Fairbanks, 1990: The Southern Oscillation recorded in the oxygen isotopes of corals from Tarawa Atoll. *Paleoceanography,* **5,** 669–683.

——, ——, and G. T. Shen, 1993: The spectrum of recent variability in the Southern Oscillation: Results from a Tarawa atoll coral. *Science,* **260,** 1790–1793.

Cole, J., R. Dunbar, T. McClanahan, and N. Muthiga, 2000: Tropical Pacific forcing of decadal SST variability in the western Indian Ocean over the past two centuries. *Science,* **287,** 617–619.

Cook, E., 2003: Reconstructions of Pacific decadal variability from long tree-ring records. *Eos, Trans. Amer. Geophys. Union,* **83,** S133.

——, and L. Kairiukstis, 1990: *Methods of Dendrochronology*. Kluwer, 394 pp.

——, D. Stahle, D. Meko, and M. Cleaveland, 1999: Drought reconstructions for the continental United States. *J. Climate,* **12,** 1145–1162.

——, R. D'Arrigo, and M. E. Mann, 2002: A well-verified, multiproxy reconstruction of the winter North Atlantic Oscillation index since A.D. 1400. *J. Climate,* **15,** 1754–1764.

D'Arrigo, R. D., G. C. Jacoby, and P. J. Krusic, 1994: Progress in dendroclimatic studies in Indonesia. *Terr. Atmos. Oceanogr. Sci.,* **5,** 349–363.

——, G. Wiles, G. Jacoby, and R. Villalba, 1999: North Pacific sea surface temperatures: Past variations inferred from tree rings. *Geophys. Res. Lett.,* **26,** 2757–2760.

——, R. Villalba, and G. Wiles, 2001: Tree-ring estimates of Pacific decadal climate variability. *Climate Dyn.,* **18,** 219–224.

——, E. Mashig, D. Frank, G. Jacoby, and R. Wilson, 2004: Reconstructed warm season temperatures for Nome, Seward Peninsula, Alaska since AD 1389. *Geophys. Res. Lett.,* **31,** L09202, doi:10.1029/2004GL019756.

Davi, N., R. D'Arrigo, G. Jacoby, B. Buckley, and O. Kobayashi, 2002: Warm-season annual temperature variability for Hokkaido, Japan reconstructed from tree-ring density data: AD 1557–1990. *Climatic Change,* **52,** 201–217.

Deser, S., A. Phillips, and J. Hurrell, 2004: Pacific interdecadal climate variability: Linkages between the Tropics and North Pacific during boreal winter since 1900. *J. Climate,* **17,** 3109–3124.

Ebbesmeyer, C., D. Cayan, D. McLain, F. Nichols, D. Peterson, and K. Redmond, 1991: 1976 step in the Pacific climate: Forty environmental changes between 1968–75 and 1977–84. *Proc. Seventh Annual Pacific Climate Workshop*, Asilomar, CA, California Dept. of Water Resources, 115–126.

Evans, M. N., M. A. Cane, D. P. Schrag, B. K. Alexey Kaplan, R. Linsley, R. Villalba, and G. M. Wellington, 2001: Support for tropically-driven Pacific decadal variability based on paleoproxy evidence. *Geophys. Res. Lett.,* **28,** 3689–3692.

Fritts, H., 1976: *Tree Rings and Climate.* Academic Press, 567 pp.

Garreaud, R., and D. Battisti, 1999: Interannual (ENSO) and interdecadal (ENSO-like) variability in the Southern Hemisphere tropospheric circulation. *J. Climate,* **12,** 2113–2122.

Gedalof, Z., and D. Smith, 2001: Interdecadal climate variability and regime-scale shifts in Pacific North America. *Geophys. Res. Lett.,* **28,** 1515–1518.

——, N. J. Mantua, and D. L. Peterson, 2002: A multi-century perspective of variability in the Pacific decadal oscillation: New insights from tree rings and coral. *Geophys. Res. Lett.,* **29,** 2204, doi:10.1029/2002GL015824.

Gordon, G., and S. LeDuc, 1981: Verification statistics for reconstruction models. Preprints, *Seventh Conf. on Probability and Statistics in Atmospheric Sciences*, Monterey, CA, Amer. Meteor. Soc., 129–133.

Graham, N., 1994: Decadal-scale climate variability in the 1970s and 1980s: Observations and model results. *Climate Dyn.,* **10,** 135–162.

——, 2004: Late-Holocene teleconnections between tropical Pacific climatic variability and precipitation in the western USA: Evidence from proxy records. *Holocene,* **14,** 436–447.

Guilderson, T. P., and D. P. Schrag, 1999: Reliability of coral isotope records from the western Pacific warm pool: A comparison using age-optimized records. *Paleoceanography,* **14,** 457–464.

Isdale, P. J., B. J. Stewart, K. S. Tickle, and J. M. Lough, 1998: Palaeohydrological variation in a tropical river catchment: A reconstruction using fluorescent bands in corals of the Great Barrier Reef, Australia. *Holocene,* **8,** 1–8.

Jacoby, G., O. Solomina, D. Frank, N. Eremenko, and R. D'Arrigo, 2004: Kunashir (Kurile Islands) oak response to temperature and relation to the Pacific Decadal Oscillation (PDO). *Palaeogeogr., Palaeoclimatol., Palaeoecol.,* **209,** 303–311.

Kaplan, A., M. Cane, Y. Kushnir, A. Clement, B. Blumenthal, and B. Rajagopalan, 1998: Analyses of global sea surface temperature 1856–1991. *J. Geophys. Res.,* **103,** 18 567–18 589.

Labeyrie, L., J. Cole, K. Alverson, and T. Stocker, 2003. The history of climate dynamics. *Paleoclimate, Global Change and the Future*, K. Alverson, R. Bradley, and T. Pederson, Eds., Springer-Verlag, 33–61.

Linsley, B. K., L. Ren, R. B. Dunbar, and S. S. Howe, 2000: El Niño–Southern Oscillation (ENSO) and decadal-scale climate variability at 10N in the eastern Pacific from 1893 to 1994: A coral-based reconstruction from Clipperton Atoll. *Paleoceanography,* **15,** 322–335.

——, G. Wellington, D. Schrag, L. Ren, M. Salinger, and A. Tudhope, 2004: Geochemical evidence from corals for changes in the amplitude and spatial pattern of South Pacific interdecadal climate variability over the last 300 years. *Climate Dyn.,* **22,** 1–11.

Mann, M. E., and J. Lees, 1996: Robust estimation of background noise and signal detection in climatic time series. *Climatic Change,* **33,** 409–445.

——, R. S. Bradley, and M. K. Hughes, 2000: Long-term variability in the El Nino Southern Oscillation and associated teleconnections. *El Niño and the Southern Oscillation: Multiscale Variability and its Impacts on Natural Ecosystems and Society*, H. F. Diaz and V. Markgraf, Eds., Cambridge University Press, 357–412.

Mantua, N., and S. Hare, 2001: The Pacific decadal oscillation. *J. Oceanogr.,* **58,** 35–44.

——, S. Hare, Y. Zhang, J. Wallace, and R. Francis, 1997: A Pacific interdecadal oscillation with impacts on salmon production. *Bull. Amer. Meteor. Soc.,* **78,** 1069–1079.

Meko, D. M., 1997: Dendroclimatic reconstruction with time varying subsets of tree indices. *J. Climate,* **10,** 687–696.

Minobe, S., 1997: A 50–70 year climatic oscillation over the North Pacific and North America. *Geophys. Res. Lett.,* **24,** 683–686.

Nakamura, H., G. Lin, and T. Yamagata, 1997: Decadal climate variability in the North Pacific during the recent decades. *Bull. Amer. Meteor. Soc.,* **78,** 2215–2225.

Percival, D., J. Overland, and H. Mofjeld, 2001: Interpretation of North Pacific variability as a short- and long-memory process. *J. Climate,* **14,** 4545–4559.

Stahle, D. W., and Coauthors, 1998: Experimental dendroclimatic reconstruction of the Southern Oscillation. *Bull. Amer. Meteor. Soc.,* **79,** 2137–2152.

Trenberth, K., 1984: Some effects of finite sample size and persistence on meteorological statistics. Part I: Autocorrelations. *Mon. Wea. Rev.,* **112,** 2359–2368.

——, and J. Hurrell, 1994: Decadal atmospheric–ocean variations in the Pacific. *Climate Dyn.,* **9,** 303–319.

Tudhope, A. W., and Coauthors, 2001: Variability in the El Nino–Southern Oscillation through a glacial–interglacial cycle. *Science,* **291,** 1511–1517.

Urban, F. E., J. E. Cole, and J. T. Overpeck, 2000: Influence of mean climate change on climate variability from a 155-year tropical Pacific coral record. *Nature,* **407,** 989–993.

Villalba, R., R. D'Arrigo, E. Cook, G. Wiles, and G. Jacoby, 2001:

Decadal-scale climatic variability along the extratropical western coast of the Americas: Evidence from tree-ring records. *Inter-Hemispheric Climate Linkages*, V. Markgraf, Ed., Academic Press, 155–172.

——, and Coauthors, 2003: Large-scale temperature changes across the southern Andes: 20th century variations in the context of the past 400 years. *Climatic Change,* **59,** 177–232.

Wiles, G., R. D'Arrigo, and G. Jacoby, 1998: Gulf of Alaska atmosphere–ocean variability over recent centuries inferred from coastal tree-ring records. *Climatic Change,* **38,** 289–306.

Yamagata, T., and Y. Masumoto, 1992: Interdecadal natural climate variability in the western Pacific and its implications on global warming. *J. Meteor. Soc. Japan,* **70,** 167–175.

Zhang, Y., J. Norris, and J. Wallace, 1998: Seasonality of large-scale atmosphere–ocean interaction over the North Pacific. *J. Climate,* **11,** 2473–2481.